Thermodynamic model of a downdraft gasifier

Thermodynamic model of a downdraft gasifier

B. Fortunato[a], G. Brunetti[b], S.M. Camporeale[c], M. Torresi[d], F. Fornarelli[e]

Department of Mechanics, Mathematics and Management
Politecnico di Bari, Via Re David, 200, 70125 Bari, Italy

[a] *bernardo.fortunato@poliba.it*
[b] *gianluigi.brunetti@gmail.com*
[c] *sergio.camporeale@poliba.it*
[d] *marco.torresi@poliba.it*
[e] *francesco.fornarelli@poliba.it*

Abstract

In this paper a fixed bed downdraft gasifier model is described, where biomass is transformed into syngas, which can be used in more efficient ways with respect to the direct combustion of biomass for generation of heat and power, and can be transported much more easily where needed. The gasification process is supposed to occur at ambient pressure using air as gasifying agent. The model has been developed and implemented by means of the computer program "Cycle Tempo" developed by TU Delft. The model is able to assess, with a good approximation, both the composition and the heating value of the syngas. A relation between the equivalence ratio, λ, and both the granulometry and the ash content of the biomass has been introduced, making more versatile the model. The gasification process involves part of the gases produced during pyrolysis. The partial combustion of these gases raises the internal temperature inducing a partial decomposition of tar. Therefore, hot gases and carbon fractions react in the reduction zone, accelerating the formation of combustible species (mainly CO and H_2). In the present gasifier model, all of the biomass gasification processes (i.e. drying, pyrolysis, oxidation and reduction) have been separately implemented. The here proposed gasifier model has been validated against several experimental data available in the literature. The model allows to reproduce with a fairly good agreement the downdraft gasifier behavior with several types of biomass, taking also into account the impact of its moisture content.

[a] *Corresponding author*

Keywords

Biomass, Syngas, Downdraft gasifier, Modelling

1 Introduction

Unlike other renewable source of energies, as wind and photovoltaics, the bio-energy sector is characterized by a high level of complexity, due to the necessary interaction with industry and the agro-forestry world. The crucial problem is the lack of a biomass market, primarily as a consequence of a scarce demand, and the lack of conversion plants arranged to use a potentially available energy source. On the supply side, notwithstanding the large amount of biomass, the high dispersion, the absence of rational and efficient systems of collection, packaging, transport and storage, the limited diffusion of technical knowledge and the high costs are the main obstacles to its widespread use. However, the use of biomass in the heat and power generation is becoming more and more common [1]-[19].

Synthetic gas (syngas), usually obtained from fossil fuels (mainly coal and natural gas), is often used as an intermediate in the production of different industrial products, such as synthetic lubrification oil and synthetic fuel via the Fischer-Tropsch process, methanol or hydrogen. However, being the biomass combustion “carbon neutral”, syngas derived from this renewable sources will have important perspectives in the next future [20]-[34]. Furthermore, the syngas is suitable to be directly used as a gaseous fuel, since it is easy to be conveyed and used in other industrial processes.

The gasification process consists in the conversion of a solid carbonaceous material, such as a biomass, in a gaseous energy carrier through a partial oxidation at high temperature [35]-[55]. The syngas produced from this process is mainly composed of carbon monoxide (CO), carbon dioxide (CO_2), hydrogen (H_2), methane (CH_4), other light hydrocarbons such as ethylene (C_2H_4) and ethane (C_2H_6), coal particles, tar and oil, nitrogen (N_2), water (H_2O). Either air, steam, oxygen or a mixture of them can be used as a gasifying agent.

The gasification process takes place within specific reactors (two examples are represented in Figure 1), through which the carbonaceous materials undergo several different sub-processes. The fundamental sub-processes are the pyrolysis and the rich combustion of the pyrolysis products.

During pyrolysis, a thermochemical decomposition of biomass occurs above the critical temperature equal to 350°C, as reported by Reed and Das [45] and the volatile components of the fuel (gaseous hydrocarbons, hydrogen, carbon monoxide, carbon dioxide, water vapor and tar) are issued. What remains after the pyrolysis process is mainly char (an agglomerate of complex nature consisting of carbon, ash, sulfur compounds and volatile hydrocarbons).

During the rich combustion of the pyrolysis products, an increase of combustible compound concentration occurs. Furthermore, there is the conversion of solid coal due to the reactions with the gasifying agent. This last stage is the most important of the entire gasification process: being the slower phase, it affects the kinetics of the entire process and, consequently, both the dimensioning and the performance of the reactor.

A first classification on the existing gasifiers considers direct and indirect gasifiers.

- Direct gasifiers burn part of the pyrolysis products, providing heat to the pyrolysis itself and for completing the gasification process.
- Indirect gasifiers perform a combustion in a separate combustion chamber and the heat is carried to the pyrolysis zone by means of a flow glowing sand or other suitable material. Indeed, the heat transport is the critical point for the development of this technology.

Additional criteria for the classification of gasifiers are the operating pressure, the gasifying agent, the type of the reactor construction. The operating pressure in indirect gasifiers is normally equal to or slightly higher than the atmospheric one, whereas in direct gasifiers the operating pressure can be significantly higher, with the advantage of a final already pressurized syngas.

The choice of the gasifying agent is a very important aspect, because the syngas characteristics depend on this choice. The composition and heating value greatly vary with the gasifying agent: air produces a low heating value syngas, in the order of 4-6 MJ/Nm^3, while, operating with pure oxygen, a syngas with a heating value comprised between 12 and 18 MJ/Nm^3 can be obtained.

Moreover, the gasifiers can be classified in: fluidized bed gasifiers [35]-[40], fixed bed gasifiers [41]-[55], bed dragged gasifiers. In turn, the fixed bed gasifiers can be distinguished in: co-current gasifiers (downdraft) and counter-current ones (updraft).

Indeed, the choice of the gasifier type depends on the characteristics of the biomass used and on the power required, which will strongly influence the cost of the entire plant. In particular, in this paper, only downdraft gasifiers have been analyzed. This kind of gasifier is usually used for the production of a syngas with a high content of volatile and a low content of tar. Downdraft gasifiers are definitely the most popular for the integration in heat and power plants.

The purpose of this study is to test the feasibility of syngas production from direct biomass gasification, building up a simple but accurate thermodynamic model able to evaluate the syngas composition and its thermodynamic properties, such as its Lower Heating Value (LHV).

2 Gasifier Models

A good and reliable theoretical model of a gasifier is a very important tool, which can give useful information for the design of this important and complex system. Many theoretical models can be found in the literature, simulating the performance of gasifiers [56]-[65] under different operating conditions (e.g., in terms of type of biomass, granulometry, moisture and ash contents). In particular, some of them use kinetic models in order to represent the biomass gasification process [61]-[65], which are suitable and accurate at moderately high temperatures ($T < 800°C$). However, they are characterized by a high level of complexity. Others apply equilibrium models for the gasification process, particularly accurate at high temperature. Equilibrium models are based either on the use of equilibrium constants or on the Gibbs free energy minimization in order to compute species concentrations at equilibrium. When equilibrium constants are considered, simple reaction mechanisms are solved, by using for input information regarding the chemical composition of the biomass. The complexity of these methods primarily depends on the number of reactions considered. In many cases, these methods can greatly simplify the analysis by using a limited number of reactions, however, compromising the reliability of the result. When the Gibbs free energy minimization is

considered, the exact knowledge of the chemical reactions mechanism is not required, allowing directly the determination of the final composition at equilibrium. Despite its simplicity, several codes, such as Cycle-Tempo [66], implement the Gibbs free energy minimization method, providing acceptable results even though not accurate enough for certain applications.

Cycle-Tempo is a software package for thermodynamic modelling and optimization of energy conversion systems, based on a modular structure. A plant can be represented by means of a set of components, including the environment, connected by pipes and ducts. The component library, available in the program, includes a large number of thermo-mechanical components (boiler, heat exchanger, turbine, compressor, pump, etc.), chemical components (combustor, gasifier, reformer, separator, fuel cell, etc.) and pipes for different operating media (refrigerants, water, steam, air, gas mixture, liquid and solid fuels, etc.). The governing system matrix to be solved is then derived by means of mass, energy and chemical species balances for each component and pipe.

The default gasifier model implemented in Cycle-Tempo have been gradually improved by the Scientific Community in order to take into account the real phenomena, occurring within the gasifier, hence improving its accuracy. For instance, Altafini et al. [41], have considered different gasifier models remarking that the trivial use of the default Cycle-Tempo gasifier module determines an under-estimation of the methane molar percentage into the syngas [41]. Altafini et al. [41], as well as Vera et al. [42], [43] and Depoorter et al. [44], suggest the following modifications:

- introduction of three different simple reactors, simulating separately pyrolysis, oxidation and reduction zones, respectively;
- separation of a fraction (5% by mass) of the inlet carbon content, in order to take into account the unavoidable losses, which occur in the gasifier due to char formation;
- bypass of a fraction of the methane formed during the pyrolysis process directly to the reduction zone outlet, in order to take into account that in a gasifier, generally, a complete equilibrium composition is not achievable.

2.1 New model developed in Cycle-Tempo

The structure of a gasifier is relatively simple, however, the development of an efficient gasification process is very complex, since a general theoretical gasification model does not exist yet. Actually, the development and the design of gasifiers are still based on empirical formulations, relying upon experimental data. These empirical formulations provide guidance on the temperature, on the air supply and on specific geometry-based parameters that depends on the gasifier layout. Most of these findings derive from testing activities not directly related to gasification, such as oil and gas combustion, however, these have contributed to a better understanding of the gasification process.

In order to set up in Cycle-Tempo [66] a simple mathematical model of a downdraft gasifier, all of the three previous suggestions have been implemented here. In particular, the present gasifier model is essentially composed of three reactors, related to pyrolysis, oxidation, and reduction, respectively, connected as shown in the complete layout (Figure 2). Each part of the model proposed in this work will be extensively described in the following subsections.

Developing the model, by using only the components available in the Cycle-Tempo library, allows one to focus its attention on the problem set up without any concern on the solution of the final problem, which is directly managed by Cycle-Tempo. The model should be robust and reliable, in order to give an accurate syngas composition, fairly evaluate the gasification cold gas efficiency, η_g, and the syngas Lower Heating Value. A robust and reliable gasifier model could be then used in the performance evaluation of thermodynamic cycles of complex plants.

In the scientific and technical literature, many models of downdraft gasifiers already exist, but, usually, they are not general and heavily depends on the specific biomass characteristics, in particular granulometry and ash content.

In the present paper a novel approach has been proposed in order to develop a more general gasifier model able to operate with different kinds of biomass, in terms of composition, granulometry and ash contents.

2.1.1 Pyrolysis

Pyrolysis is a thermochemical decomposition of organic materials in absence of oxygen. This is the first step of the biomass gasification: when the biomass is heated up above 350°*C* (as indicated by Reed and Das in their Handbook of Biomass Downdraft Gasifier Engine Systems [45]) in absence of oxygen, it partially devolatilizes, producing both gas (CO, CO_2, H_2, H_2O, CH_4) and vapor (mainly tar, consisting of various heavy organic compounds), leaving a solid residue characterized by a high carbon content (char). Cooling down the devolatilized products, the vapor fraction condenses, diminishing the tar content. The heat flux necessary to sustain the pyrolysis, is usually generated by the combustion of a fraction of the volatile products in the oxidation and reduction zones.

In order to set up the model, the initial biomass taken into account is depleted pomace, having the composition shown in Table 1.

A mass flow rate equal to 0.15 kg/s of depleted pomace at 20°C is fed by means of *source 1* as reported both in Figure 2 and Figure 3.

The pomace Lower Heating Value (LHV) has been calculated according to the Boie formula [67]:

$$LHV_{pomace} = 34.8\,C + 93.9\,H + 6.3\,N + 10.5\,S - 10.8\,O - 2.44\,W\ (MJ/kg)$$

based on the biomass ultimate analysis, which gives the composition of the biomass in wt% of carbon, *C*, hydrogen, *H*, nitrogen, *N*, sulfur, *S*, oxygen, *O*, and moisture, *W*.

Figure 3 shows the first part of the gasifier scheme, containing the pyrolysis module (*gasifier 2*). From *source 1*, the biomass is fed into *gasifier 2* through *duct 3*, where, providing air (*source 5*) with an air/fuel ratio, $\alpha = 0.018$, and allowing a heat exchange (by means of *heat exchanger 2*), the pyrolysis process can be sustained at 600°*C*. From *source 4*, a water flow goes through the *heat exchanger*. The inlet and outlet temperatures of the water flow are known, hence the software can compute the mass flow rate satisfying the heat power requirement for the pyrolysis. The use of the water flow in the heat exchanger is only an artifice in order to allow the heat transfer between the pyrolysis zone (*gasifier 2*) and the reduction zone (*gasifier 17*, in Figure 2), where another *heat exchanger* brings back the water flow to its initial condition at *sink 18*. In this way, the thermal power needed by pyrolysis is actually

absorbed from the reduction zone, which is maintained at 850°*C*. The process temperatures for both pyrolysis (600°*C*) and reduction (850°*C*) have been chosen according to the results contained in the Handbook of Biomass Downdraft Gasifier Engine Systems [45] and in the work of Chao and Yuping [68]. In the latter, the authors equipped their gasifier with thermocouples, even in the vicinity of the reduction plate. The temperature of the outlet gas from the reduction zone is then computed and depends also on the heat absorbed in the pyrolysis process. For both pyrolysis and reduction zones (modules 2 and 17, respectively) a power loss, accounting for the heat exchange toward the environment, is considered and quantified as 0.5% each (12.5kW) of the input biomass heat rate (2.53MW). Actually, the pyrolysis model cannot guaranty an accurate assessment of the pyrolysis products, however the aim of the model is to accurately assess only the final composition of the syngas.

Through *duct* 5, pyrolysis products reach *separator 6*, where they are split toward the oxidation and reduction zones. In particular, the solid fractions (coal and ash) are entirely conveyed by means of *duct 6*, together with an 80% by mass of the methane produced during pyrolysis. This value of the bypassed fraction of methane is a characteristic value imposed in the proposed model, for the sake of simplicity. Therefore, the final value of methane in the syngas is only affected by the composition of the biomass that will determine the amount of methane produced during pyrolysis.

It is well known that the presence of coal is normal: in fact in a downdraft gasifier, part of the biomass, varying from 10% to 20% , remains in the form of coal after the pyrolysis. Moreover, according to Vera et al. [42], [43], in the s*eparator 7*, ash and a 5% by mass of coal are removed flowing in *sink 8* . This represents the effect of the non-reacting coal, following the formation of char during the gasification process. The remaining part is conveyed with the bypassed fraction of methane through *duct 13* (see details in Figure 3).

2.1.2 Oxidation

As shown by Altafini et al. [41], Vera et al. [42] and Depoorter et al. [44], in order to improve the accuracy of the gasifier model, an oxidation zone is introduced, in which high temperatures can be

reached, where the cracking of the tar produced during pyrolysis can occur. This process is shown schematically in Figure 4.

Pyrolysis products are partially conveyed by means of an ejector towards a combustion chamber, without the solid fraction, where a complete combustion occurs at high temperature. The hot combustion products are then injected in the middle of the gasifier to ensure the heat supply for pyrolysis and gasification of the solid fraction. Then, the high temperatures promote the destruction of tar.

Therefore, the gas output from *separator 6*, through *duct 8*, crosses *splitter 9*, which divides the gas stream into two equal parts, through the *ducts 9* and *12*, which will be re-joined in the *node 12*.The gas in *pipe 9* reaches *combustor 10*, which represents the oxidation zone. Then an air mass flux, previously heated up at 200°C [41] by the syngas, exiting the gasifier (*node 20*), is insufflated with an equivalence ratio $\lambda = \alpha/\alpha_{st} = 2$, reaching a reaction temperature equal to 1440°C. The hot combustion products reach *node 12*, where they are mixed together with the mass flux coming from *duct 12*, generating a mass flux at 1269°C. As suggested by Altafini et al [41], a fictitious heat exchanger (*module 13*) allows the combustion gases to heat the coal, coming from *separator 23*, up to 700°C (Figure 4).

2.1.3 Reduction

In a real reactor, the presence of methane in the gasification products is due to the reaction between CO and H_2, called methanation [45], which takes place if the temperature is maintained below 900°C in the reduction zone:

$$CO + 3H_2 \rightarrow CH_4 + H_2O$$

This reaction proceeds slowly in the absence of a catalyst and it is not contemplated in the commonly used thermodynamic models. Usually, these mathematical models assume that the reactions occur in thermodynamic equilibrium, condition that the pyrolysis products would attain in the reduction zone before leaving the gasifier. Moreover, these models, are based on the Gibbs free energy minimization principle in order to compute chemical species concentration at equilibrium, as it is reported in Zainal

et al. [59] and in Altafini et al. [41]. This approach strongly underestimates the percentage of methane in the syngas and it overestimates the hydrogen concentration. Therefore, in order to obtain the right methane concentration in the syngas, a fictitious bypass of both oxidation and reduction stages by the methane produced during pyrolysis is needed. This bypass is performed by means of two *separators* (*23* and *14*) as shown in Figure 4. *Separator 23* subtracts all the methane contained in the stream of *duct 13* (i.e. 80% by mass of CH_4 produced during pyrolysis), channeling it into *duct 22*, which ends into *node 24*. *Separator 14*, already introduced in the study of Altafini et al. [41], subtracts all the methane contained the stream of *duct 15*, channeling it to *node 24.* In this way, methane bypasses *gasifier 17* (Figure 5), and it is mixed with the reduction products in *node 20*.

Finally, after the methane spillover, coal at 700°C is mixed in *node 15* with the hot gas, exiting *separator 14* (current in the *duct 17*), and it reaches *gasifier 17*, where the reduction zone at 850°C is simulated. The gas, exiting the reduction zone, is enriched of methane in *node 20*, giving the final syngas composition. This flow is then used to preheat the combustion air and finally is sent to the cooling and depuration systems. The scheme of the last part of the process is shown in Figure 5.

2.2 Differences with respect to the model of Altafini et al.

The basic idea of splitting a gasifier process with three different Cycle Tempo modules, proposed in this paper, has been derived from the work of Altafini et al. [41]. However, there are many important differences between these two models. The main differences are here reported and they can be verified looking at the layout of Altafini et al. reproduced in Figure 6.

- Heat flux to sustain the pyrolysis. In the present model, air is not considered in both pyrolysis and reduction reactors. Therefore, heat is transferred from the reduction zone to the pyrolysis zone, via a water flux and two fictitious heat exchanger. In the Altafini's model, heat is generated by chemical reactions in both pyrolysis and reduction reactors, which need specific air mass flow inlets (for the combustion process). Moreover, even in the Altafini's model, there is the air mass flow inlet (*module 7*) related to the oxidation process. All of these air inlets have to be quantified separately for each kind of biomass used in the plant. In the present model,

when pyrolysis is considered, only a mass flow rate almost equal to zero (0.003 kg/s) is taken into account and its value is the same for any kind of biomass used in the gasifier. Furthermore, the air mass flow inlet in the oxidation reactor is calculated by the software on the basis of the equivalence ratio, λ, which is given as an input, according to the granulometry and ash content of the gasified biomass, as will be shown later in this paper. In this way, this approach allows the model to analyze the gasification process for different types of biomass imposing only the biomass characteristics;

- Separation of methane CH_4. In the Altafini's model, the methane bypass is performed by means of only one module (*module 11*), whereas in the present model three different modules (*6*, *23* and *14*) are involved, allowing a good agreement with respect to experiments in terms of CH_4 content.
- Air preheating phase. This is not considered by Altafini et al.;
- Syngas depuration. This is not considered by Altafini et al.

Finally, the key feature in the biomass gasification modeling proposed in this paper is represented by its capability in the prediction of the syngas characteristics (e.g. species concentrations and lower heating value) independently from the biomass and, particularly, from its granulometry and from its ash content, finding a good approximation in the results.

3 Validation of the model

As reported in the scientific literature, a downdraft gasifier is not very versatile because it cannot be used with many different types of biomass. In fact, a gasifier is usually designed *ad hoc* according to the physical and chemical characteristics of the selected biomass to be used.

The downdraft gasifier model here presented has been developed in order to well simulate the syngas production of an Ankur gasifier [43], which can be fed with pomace, leaves and pruning, olive pits prepared with a granulometry variable from 10 to 50 mm, an ash content lower than 5%, and a moisture lower than 20%.

In Table 2, the characteristics of the syngas derived from pomace obtained with the present model (FB downdraft column) are compared with experiments [43] and with those theoretically obtained by Vera et al. [43]. The syngas composition obtained with the present model is very close to that measured during the experiments. A slight difference can be found in the air/fuel ratio, α, that is higher than the one measured in the experiment.

Then, the cold-gas efficiency, η_g, has been calculated:

$$\eta_g = \left(G_{syn} LHV_{syn}\right)/(G_b LHV_b) = 0.76$$

where *syn* refers to syngas and *b* to biomass.

Several numerical simulations have been also carried out in order to assess the impact of the biomass moisture content on the final syngas composition. The moisture content of the exhausted pomace has been gradually increased (10%, 15% and 20%), reporting the results in Table 3 and graphically in Figure 7, where it can be observed:

- a constant increase in the air/fuel ratio;
- a little change in the syngas hydrogen content;
- a significant increase in the CO content, responsible for the decrease in the LHV (Figure 7/a);
- a constant increase in the percentage of CO_2 and N_2 in the syngas;
- a reduction in the cold-gas efficiency (Figure 7/b).

Moreover, the validation phase has been carried out also by evaluating the change in the syngas characteristics (composition, LHV, air/fuel ratio, cold-gas efficiency) when other types of biomass are considered, namely, leaves and pruning residues and olive pits (woody biomass for which the Ankur gasifier was designed). The comparison has been performed against the experimental data of the Ankur gasifier and the theoretical results available in the work of Vera at al. [43]. Details of the compositions of both leaves and pruning residues and olive pits are given in Table 4. Without any modification of the operating parameters, the results show a good agreement with the experimental data, as reported in Table 5. Despite a slight overestimation of the molar percentages of CO in the syngas, a very good agreement of the final syngas characteristics with respect to the measured data can

be recognized. Valuable is the improvement with respect to the model of Vera et al. [43] in the estimation of the methane percentage in the syngas, which is very close to 3%.

4 Influence of biomass granulometry and ash content

By building the present gasification model, the authors have tried to overcome the limiting hypotheses on the biomass characteristics (mainly granulometry ash content, and moisture), in order to compare its results with a wide range of experimental data from other gasifiers.

4.1 Determination of the equivalence ratio

As previously depicted, the oxidation step in the gasification process is simulated by means of a combustor. The equivalence ratio, λ, is calculated from the analysis of various data available in the literature. In particular, with reference to the previous validation study on the Ankur gasifier [43], the equivalence ratio, λ, has been evaluated to be equal to 2, considering the biomass characteristics (variable granulometry from 10 to 50 mm and an ash content lower than 5%).

The validation of the model has been performed by choosing the process parameters and in particular the equivalence ratio, λ. The model can be tuned adjusting only the equivalence ratio, λ, according to the biomass characteristics in terms of granulometry, ash content and moisture.

As shown by Pérez et al. [69], there are many parameters that affect the gasification process, in particular:

- the increase of the reactor dimensions determines an increase of the flame speed, the consumption of biomass, the relationship between the equivalence ratio and the quality of the obtained syngas;
- the content of volatile matter affects the flame speed and the generation of thermal power;
- the increase of moisture together with the increase of the granulometry determines the reduction of the flame speed, the consumption of biomass and the equivalence ratio.

Indeed, the use of a thermodynamic model makes difficult the description of the physical mechanisms that influence the results. Therefore, the use of a kinetic model would be more suitable, but more complex in terms of computational effort.

These effects on the gasification model have been initially tested retaining the settings in the various program modules. However, the modification of the biomass (e.g. sawdust, RDF, sewage sludge) affected the performance with a reduction in accuracy, predicting the syngas characteristics in comparison to the experimental data. Therefore, it was necessary to introduce an empirical method able to correct some of the parameters of the model. Our attention was focused on the equivalence ratio, λ. We supposed that the equivalence ratio, λ, depends on the biomass average particle diameter, D, and the biomass ash content, C:

$$\lambda = 2(1 + \Delta\lambda_{ash} + \Delta\lambda_{diam}) \tag{1}$$

where $\Delta\lambda_{ash}$ is the change in λ due to the variation in the ash content, C, with respect to the value allowed by the Ankur gasifier model, given by:

$$\Delta\lambda_{ash} = K_1 x \tag{2}$$

and $\Delta\lambda_{diam}$ is the change in λ due to the variation of the average particle diameter, D, with respect to the value allowed by the "Ankur" model, given by:

$$\Delta\lambda_{diam} = K_2 y \tag{3}$$

K_1 and K_2 being constant to be determined and x and y defined as follows:

$$x = \begin{cases} 0 & C \leq 5\% \\ \frac{C-5}{5} & C > 5\% \end{cases} \tag{4}$$

$$y = \begin{cases} \frac{10-D}{10} & D < 10mm \\ 0 & 10mm \leq D \leq 50mm \\ \frac{D-50}{50} & D > 50mm \end{cases} \tag{5}$$

In Figure 8, the equivalence ratio, λ, is reported as function of the ash content, C, for different values of the average particle diameter, D.

At last, in Figure 9, the equivalence ratio, λ, is reported as function of the average particle diameter, D, for different values of the ash content, C.

In order to evaluate the K_1 and K_2 constants, sludge purification and sawdust biomass have been exploited. The first one, in fact, has an ash content higher than 5% related to the biomass used in the Ankur gasifier, but is prepared in compatible grain size. The sawdust, instead, has a low ash content, but is normally constituted by particles with a diameter of about 2-3 mm.

Kept constant the pyrolysis conditions, in both cases, it was decided to proceed by varying the equivalence ratio, λ, in the oxidation module until the achievement of a compatible syngas composition with respect to experimental data. The two values selected are the followings (Table 6):

$$\lambda_{sludge} = 2.6 \tag{6}$$

$$\lambda_{sawdust} = 2.36 \tag{7}$$

From equation (1), we obtained:

$$\lambda_{sludge} = 2\left(1 + \Delta\lambda_{ash,sl} + \Delta\lambda_{diam,sl}\right) = 2\left(1 + \Delta\lambda_{ash,sl} + 0\right) = 2.6 \tag{8}$$

$$\lambda_{sawdust} = 2\left(1 + \Delta\lambda_{ash,saw} + \Delta\lambda_{diam,saw}\right) = 2\left(1 + 0 + \Delta\lambda_{diam,saw}\right) = 2.36 \tag{9}$$

Hence, the values of $\Delta\lambda_{ash,sl}$ and $\Delta\lambda_{diam,saw}$ can be evaluated:

$$\Delta\lambda_{ash,sl} = 0.3 \tag{10}$$

$$\Delta\lambda_{diams,aw} = 0.18 \tag{11}$$

Finally, the K_1 and K_2 constants can be derived from equations (2) and (3) and values (10) and (11):

$$K_1 = \frac{30}{314.6} \tag{12}$$

$$K_2 = \frac{18}{80} \tag{13}$$

4.2 Syngas from sawdust

In the hypothesis of gasifying the sawdust, the syngas characteristics, obtained by the proposed model, have been compared with those obtained experimentally. The properties of the biomass are shown in

Table 7. The characteristics of the experimental reactor are given by Altafini et al. [41], and the results are visible in Table 8.

From the comparison between theoretical and experimental results, a good approximation of the theoretical composition of the synthesis gas appears. The Higher Heating Value (HHV) is well estimated. However, these results have been obtained using an equivalence ratio, $\lambda = 2.07$, that is higher than the experimental one equal to 1.829. Such discrepancy is due to some settings of the model, which operates with a constant conversion efficiency of coal equal to 95% (an optimistic value for small size gasifiers). For the same reason there is also a sensible difference in the cold gas efficiency.

4.3 Syngas from sewage sludge

In the hypothesis of gasifying the sewage sludge, the syngas characteristics, obtained by the proposed model, have been compared with those obtained experimentally. The properties of the biomass are shown in Table 9. The characteristics of the experimental reactor are given by Dogru et al. [46], and the results are visible in Table 10. The λ_{sludge} evaluated by the previous analysis is 2.6. A slight overestimation of the methane percentage compared to experimental data has been found, while the HHV is provided with sufficient approximation. There is still a discrepancy in the equivalence ratio, this time under-estimated with respect to the one used during the experiments, again influencing the cold gas efficiency.

4.4 Syngas from RDF

Previously, the syngas compositions have been obtained from sawdust and sewage sludge, represented respectively in Table 8 and Table 10. The variation of the equivalence ratio, λ, is related to the variation of both mean particle diameter, D, and ash content, C, with respect to standard values: $D_{standard} = 10 - 50\ mm$ and $C_{standard} = 5\%$. In Table 6, it can be noted that a reduction of 80% of the diameter corresponds to an 18% increase of λ and an increase of 314.6% of the ash content corresponds to a 30% increase of λ.

With reference to RDF biomass, characterized by high ash content and by reduced granulometry (see Table 11 for the RDF physical properties), the λ value has been evaluated according to the present model.

From Equation (2) and (3), the following relation can be obtained:

$$\Delta\lambda_{ash,RDF} = K_1 x_{RDF} \tag{14}$$

$$\Delta\lambda_{diam,RDF} = K_2 y_{RDF} \tag{15}$$

whereas x_{RDF} and y_{RDF} values can be evaluated according to equations (4) and (5), once the values of the corresponding mean particle diamenter, D_{RDF}, and ash content, C_{RDF}, are considered (Table 11).

$$\lambda_{RDF} = 2\left(1 + \Delta\lambda_{ash,\mathrm{RDF}} + \Delta\lambda_{diam,\mathrm{RDF}}\right) = 2.37 \tag{16}$$

Starting from an RDF, whose characteristics are given in Table 12, the results shown in Table 13 have been obtained. These results have been compared with those taken from the literature and regarding urban solid waste [55] (see Table 9). There is a substantial difference in the prediction of the molar percentages of both methane and hydrogen in the syngas, however a good agreement in terms of the other chemical species.

The under-estimation of the molar percentage of methane and the over-estimation of the molar percentage of hydrogen could be imputed to the Gibbs free energy minimization method, which the Cycle Tempo software relies on. Actually, the Gibbs free energy minimization method do not consider each single step of the methanation reactions neither all of the other reactions involving hydrocarbons, C_mH_n, (e.g. the reactions in Angelova et al. [55]), but only a single global reaction. This is the reason why, we introduced the recirculation of the 80% by mass of the CH4 produced during pyrolysis directly downstream the reactor. For instance, also Zainal et al. [59] and Altafini et al. [41] obtained the same behavior with their models.

4.5 Syngas from corn straw

Similarly, the calculation of the λ parameter for a biomass consisting of corn straw, whose properties are reported in Table 14 and Table 15 have been performed as follows:

$$\Delta\lambda_{ash,\mathrm{cs}} = 0.0177 \tag{17}$$

$$\Delta\lambda_{diam,cs} = 0.14 \tag{18}$$

$$\lambda_{cs} = 2\left(1 + \Delta\lambda_{ash,\mathrm{cs}} + \Delta\lambda_{diam,\mathrm{cs}}\right) = 2.32 \tag{19}$$

With these parameters, the syngas composition has been evaluated, and then the results compared with the experimental data obtained by Chao and Yuping [68] as reported in Table 16.

The obtained syngas composition is close to the average values obtained in the experimental data, showing again the validity of the present approach.

5 Cooling system and purification of gas

Usually, the syngas produced in a gasifier contains unwanted and potentially harmful constituents, among others:

- Particles (dust, char, ash), which could be dragged in suspension in the syngas, causing erosion and clogging, e.g. on guide vanes or rotor blades;
- Alkali metals (mainly Na and K), which can cause corrosion at high temperature;
- Nitrogen compounds (e.g. NH_3 and HCN), which can contribute to NOx formation during the syngas combustion;
- Tar (a mixture of long-chain hydrocarbons), which can condense in the form of aerosols below 300-400°C, generating fouling in the guide vanes or rotor blades of compressors and turbines;
- Sulfur and chlorine compounds (H_2S, HCl), which can cause acid corrosion.

The purification of the syngas, therefore, will be fundamental for all those cases in which the direct combustion at the exit of the gasifier is expected. Specifically, the system that has been simulated (Figure 10), consists in a module for filtering particles and powders (*module 34*), followed by Venturi scrubbers (*modules 16* and *3*).

The Venturi scrubber is particularly suitable for the treatment of highly soluble acid compounds and it is simulated in the software “Cycle-Tempo” by means of a simple separator module, used for the removal of selected substances, and a parallel flow saturator. Finally, the gas is dehumidified through a condensate separation module (*module 26*), from which the syngas flows out at a temperature of

30°C. In this case, a possible tar treatment has been neglected. However, in a downdraft gasifier with combustion chamber, the tar content is negligible in the syngas. The composition of the purified syngas, derived by exhaust pomace, is reported in Table 17.

Conclusions

In this paper a thermodynamic model to evaluate the performance of a downdraft gasifier has been presented. The model has been built using the computer program "Cycle Tempo" developed by TU Delft, with a modular structure based on linked objects. Even though the software already includes a standard gasifier model, which compute the final syngas composition (based on the minimization of the Gibbs free energy), this actually under-estimates the molar fraction of methane in the syngas. For this reason, a more complex thermodynamic model of a downdraft gasifier has been built in the Cycle Tempo environment. In order to describe the gasification process, the proposed thermodynamic model is based on three separated reactors, simulating each one pyrolysis, oxidation and reduction, respectively. Moreover, it includes a partial extraction of the initial carbon content (5% by mass) for the formation of char, and a partial extraction of methane, produced during the pyrolysis phase, bypassing the reduction zone, in order to guaranty the correct syngas composition. The model has been applied to several type of biomass, showing a good agreement with respect to experimental data available in the literature.

In the case of using exhaust pomace as biomass input, the results have been compared against the characteristics of syngas obtained with an Ankur gasifier [43]. The syngas composition and the cold-gas efficiency, η_g, were very close to the experimental measurements. In the numerical simulations, the impact of the moisture content in the biomass (10%, 15%, 20%) on the gasification process has been also taken into account. Furthermore, the model has been used also in the case of gasifying "leaves and pruning" and "olive pits" in the same plant, showing again a good agreement.

In order to improve generality and reliability of the model with respect to different types of inlet biomass, an empirical method to evaluate the excess air ratio, λ, as function of particle size and ash content has been proposed. Thus, sludge purification and sawdust biomass have been considered.

Actually, the former has an ash content higher than that obtained in the Ankur gasifier, however has a compatible grain size. The latter, even if it has a lower ash content, is constituted by particles with a diameter of about 2-3 mm. In both cases, simulations have been performed maintaining constant the pyrolysis conditions, whereas the excess air ratio, λ, in the combustion zone has been changed until results, compatible with the experimental data, were reached. For all of the test cases considered in this work, the syngas compositions predicted by means of the proposed gasifier model are always close to the mean values obtained in the experiments. Finally, two modules have been added for the cooling system and the gas purification, respectively. The results have shown that the proposed model could be suitably used in the analysis of complex energy systems. For instance, the integration of the proposed gasifier model in the simulation of combined cycles, using either internal or external combustion systems fueled by different kinds of syngas obtained from waste biomass, or in co-firing systems, appears to be promising.

Acknowledgements

The authors would like to thank the Energy Technology Section of the TU Delft University for licensing a copy of Cycle-Tempo.

References

[1] Fortunato B, Camporeale SM, Torresi M, Fornarelli F, Brunetti G, Pantaleo AM., (2016). A combined power plant fueled by syngas produced in a downdraft gasifier. In: Proceedings of the ASME Turbo Expo 2016, 3, Seoul, South Korea, June 13–17, 2016 - GT2016-58159.

[2] Jablonski S, Pantaleo AM, Panoutsou C, Bauen A, (2006). Where can bioenergy heat applications be the most suitable? A market segmentation analysis of the UK heat market. In: Proceedings of Annual British Institute of Energy Economics Conference, Oxford, UK, 20-21 September 2006.

[3] Pantaleo AM, Tiravanti G, Bauen A, Howekes A, (2006). Overview and techno-economic assessment of small scale bioenergy CHP plants in the Italian and UK energy markets. In:

Proceedings of Cambridge Symposium on decentralized generation, Cambridge, UK, 28 september 2006.

[4] Tiravanti G, Pantaleo AM, Fanelli A, Candelise C, (2007). Investments in energy saving measures in Italy and UK: the impact of national support schemes on the business strategies of an ESCO. In: Proceedings of ECEEE Summer Study, 4-7/06/2007, Nice, France (peer reviewed paper), ISBN: 978-91-633-0899-4.

[5] Pantaleo AM, Tiravanti G, Pellerano A, (2007). Pellets production routes: overview and techno-economic study in Southern Italy. 15th European Biomass Conference and Exhibition from research to market deployment, Berlin 7-11/05/2007, ISBN: 978-88-89407-59-X.

[6] Pantaleo AM, Jablonski S, Panoutsou C, Bauen A, (2007). Assessment of the potential bioenergy demand for electricity and CHP: the case of the UK. 15th European Biomass Conference and Exhibition from research to market deployment, Berlin 7-11/05/2007, ISBN: 978-88-89407-59-X.

[7] Pantaleo AM, Tiravanti G, Bauen A, Pellerano A, (2007). Small scale bioenergy CHP technologies in the UK and Italian market. 15th European Biomass Conference and Exhibition from research to market deployment, Berlin 7-11/05/2007, ISBN :978-88-89407-59-X.

[8] Tenerelli P, Pantaleo AM, Carone MT, Pellerano A, Recchia L, (2007). Spatial, environmental and economic modelling of energy crop routes: liquid vs solid biomass to electricity chains in Puglia region. 15th European Biomass Conference and Exhibition from research to market deployment, Berlin 7-11/05/2007 ISBN 978-88-89407-59-X.

[9] Jablonski S, Pantaleo AM, Panoutsou C, Bauen A, (2007). Assessment of the potential bioenergy demand for heat, and combined heat and power: the case of the UK residential heat sector. 15th European Biomass Conference and Exhibition from research to market deployment, Berlin 7-11/05/2007, ISBN 978-88-89407-59-X.

[10] Jablonski S, Pantaleo AM, Bauen A, Pearson P, Panoutsou C, Slade R, (2008). The potential demand for bioenergy in residential heating applications (bio-heat) in the UK based on a market segment analysis. Biomass and Bioenergy, 32(7), 635-653

[11] Alkhamis TM, Kablan MM, (1999). Olive cake as an energy source and catalyst for oil shale production of energy and its impact on the environment. Energy Conversion and Management 40, 1863-1870.

[12] Camporeale SM, Fortunato B, Pantaleo AM, Sciacovelli D, (2011). Biomass utilization in dual combustion gas turbines for distributed power generation in Mediterranean countries. Proceedings of ASME Turbo Expo 2011, June 6-10, 2011, Vancouver, British Columbia, Canada, GT2011-45727.

[13] Fortunato B, Camporeale SM, Torresi M, (2013). A gas-steam combined cycle powered by syngas derived from biomass. Procedia Computer Science, 19, 736-745.

[14] Van Loo S, Koppejan J, (2008). The handbook of biomass combustion and co-firing, Ed. London, Sterling, VA, Earthscan, 2008.

[15] Wang J, Yang Y, (2016). Energy, exergy and environmental analysis of a hybrid combined cooling heating and power system utilizing biomass and solar energy. Energy Conversion and Management, 124, 566-577.

[16] Wang J, Mao T, Sui J, Jin H, (2015). Modeling and performance analysis of CCHP (combined cooling, heating and power) system based on co-firing of natural gas and biomass gasification gas. Energy, 93, 801-815.

[17] Chaves LI, da Silva MJ, de Souza SNM, Secco D, Rosa HA, Nogueira CEC, Frigo EP, (2016). Small-scale power generation analysis: Downdraft gasifier coupled to engine generator set. Renewable and Sustainable Energy Reviews, 58, 491-498.

[18] Camporeale SM, Ciliberti PD, Fortunato B, Torresi M, Pantaleo AM, (2017). Externally Fired Micro-Gas Turbine and Organic Rankine Cycle Bottoming Cycle: Optimal Biomass/Natural Gas Combined Heat and Power Generation Configuration for Residential Energy Demand, Journal of Engineering for Gas Turbines and Power, 139(4), art.no. 041401.

[19] Camporeale SM, Fortunato B, Torresi M, Turi F, Pantaleo AM, Pellerano A, (2015). Part load performance and operating strategies of a natural gas-biomass dual fueled microturbine for

combined heat and power generation. Journal of Engineering for Gas Turbines and Power, 137(12), art.no. 121401.

[20] Pantaleo AM, Pellerano A, Carone MT, (2009). Potentials and feasibility assessment of small scale CHP plants fired by energy crops in Puglia region (Italy), Biosystems Engineering, 102(3).

[21] Caputo AC, Scacchia F, Pelagagge PM, (2003). Disposal of by-products in olive oil industry: waste-to-energy solutions. Applied Thermal Engineering, 23, 197-214.

[22] Pantaleo AM, Pellerano A, Trovato M, (2002). Impact of environmental externalities on the competitiveness of biomass power plants. In: Proceedings of the 12th European Conference and Technology Exhibition on Biomass for Energy, Industry and Climate Protection, Amsterdam, 17-21/06/02, ETA-Florence, pp 1300-1305, ISBN 88-900442-5-X.

[23] Hosseini SE, Wahid MA, Ganjehkaviri A, (2015). An overview of renewable hydrogen production from thermochemical process of oil palm solid waste in Malaysia. Energy Conversion and Management, 94, 415-429.

[24] Tapasvi D, Kempegowda RS, Tran K-Q, Skreiberg Ø, Grønli M, (2015). A simulation study on the torrefied biomass gasification. Energy Conversion and Management, 90, 446-457.

[25] Sharma S, Sheth PN, (2016). Air–steam biomass gasification: Experiments, modeling and simulation. Energy Conversion and Management, 110, 307-318.

[26] Sepe AM, Li J, Paul MC, (2016). Assessing biomass steam gasification technologies using a multi-purpose model. Energy Conversion and Management, 129, 216-226.

[27] Pantaleo AM, Pellerano A, (2005). Biomass energy surveying and techno-economical assessment of suitable CHP plants: an application to Basilicata Region. Rivista di Ingegneria Agraria, No 2, 27-36.

[28] Bridgwater AV, Double JM, (1991). Production costs of liquid fuel from biomass. Fuel, 70(10), 1209–24.

[29] Dong Y, Steinberg M, (1997). Hynol-An economic process for methanol production from biomass and natural gas with reduced CO emission. International Journal of Hydrogen Energy, 22(10–11), 971–7.

[30] Hamelinck CN, Faaij APC, (2002). Future prospects for production of methanol and hydrogen from biomass. Journal of Power Sources, 111(1), 1–22.

[31] Chmielniak T, Sciazko M (2003). Co-gasification of biomass and coal for methanol synthesis. Applied Energy, 74, 393-403.

[32] Tijmensen MJA, Faaij APC, Hamelinck CN, van Hardeveld MRM, (2002). Exploration of the possibilities for production of Fischer–Tropsch liquids and power via biomass gasification. Biomass Bioenergy, 23(2), 129–52.

[33] Faaij A, Hamelinck C, Tijmensen M, (2001). Long term perspectives for production of fuels from biomass; integrated assessment and R&D priorities – preliminary results. In: Kyritsis S et al., editors. In: Proceedings of the first world conference on biomass for energy and industry. Sevilla, James & James (Science Publisher) Ltd.

[34] Larson ED, Jin H, (1999). Biomass conversion to Fischer-Tropsch liquids: preliminary energy balances. In: Proceedings of the 4th biomass conference of the Americas. Oakland, CA, Aug. 29-Sept. 2, 1999

[35] Arena U, Di Gregorio F, Mastellone ML, Zaccariello L, (2010). Fluidized bed gasification of a natural biomass: a process performance comparison of two design configurations. Processes and Technologies for a Sustainable Energy, Ischia, Italy, June 27-30, 2010.

[36] Bridgwater AV, (1995). The technical and economic feasibility of biomass gasification for power generation. Fuel, 74(5), 631-653.

[37] Hofbauer H, Rauch R, Loeffler G, Kaiser S, Fercher H, Tremmel H, (2002). Six years experience with the FICFB-gasification process. In: Proceedings of the 12th European Biomass Conference, Florence, Italy, 982-985.

[38] Schuster G, Loffler G, Weigl K, Hofbauer H, (2001). Biomass steam gasification - an extensive parametric modeling study. Bioresource Technology, 77, 71-79.

[39] Warnecke R, (2000). Gasification of biomass: comparison of fix bed or fluidized bed gassifier. Biomass and Bioenergy, 18, 489-497.

[40] Fanelli E, Canneto G, Nanna F, Braccio G, Freda C, (2009). Theoretical model validation of a steam-oxygen fluidized bed gasifier for gas turbine application. In: Proceedings of the 17th European Biomass Conference and Exhibition. From Research to Industry and Market, Hamburg, Germany.

[41] Altafini CR, Wander PR, Barreto RM, (2003). Prediction of the working parameters of a wood waste gasifier through an equilibrium model. Energy Conversion and Management, 44, 2763–277

[42] Vera D, de Mena B, Jurado F, Schories G, (2013). Study of a downdraft gasifier and gas engine fueled with olive oil industry wastes, Applied Thermal Engineering, 51, 119-129

[43] Vera D, Jurado F, Carpio J, (2011). Study of a downdraft gasifier and externally fired gas turbine for olive oil industry wastes. Fuel Processing Technology 92, 1970-1979

[44] Depoorter V, Olivella-Rosell P, Sudrià-Andreu A, Jordi Giral-Guardia J, Sumper A, (2014). Simulation of a small-scale electricity generation system from biomass gasification. Renewable Energy and Power Quality Journal, (RE&PQJ) ISSN 2172-038 X, No.12

[45] Reed TB, Das A, (1988). Handbook of Biomass Downdraft Gasifier Engine Systems. SERI/SP-271-3022, DE88001135, March 1988, UC Category: 245

[46] Dogru M, Midilli A, Howarth CR, (2002). Gasification of sewage sludge using a throated downdraft gasifier and uncertainty analysis, Fuel Processing Technology, 75, 55–82.

[47] Minutillo M, Perna A, Di Bona D, (2009). Modelling and performance analysis of an integrated plasma gasification combined cycle (IPGCC) power plant. Energy Conversion and Management, 50, 2837–2842.

[48] Rong L, Maneerung T, Ng JC, Neoh KG, Bay BH, Tong YW, Dai Y, Wang C-H, (2015). Co-gasification of sewage sludge and woody biomass in a fixed-bed downdraft gasifier: Toxicity assessment of solid residues. Waste Management, 36, 241-255.

[49] Roy PC, Datta A, Chakraborty N, (2013). An assessment of different biomass feedstocks in a downdraft gasifier for engine application. Fuel, 106, 864-868.

[50] Itai Y, Santos R, Branquinho M, Malico I, Ghesti GF, Brasil AM, (2014). Numerical and experimental assessment of a downdraft gasifier for electric power in Amazon using açaí seed (Euterpe oleracea Mart.) as a fuel. Renewable Energy, 66, 662-669.

[51] Patra TK, Sheth PN, (2015). Biomass gasification models for downdraft gasifier: A state-of-the-art review. Renewable and Sustainable Energy Reviews, 50, 583-593.

[52] Ingle NA, Lakade SS, (2016). Design and Development of Downdraft Gasifier to Generate Producer Gas. Energy Procedia, 90, 423-431.

[53] Chaurasia A, (2016). Modeling, simulation and optimization of downdraft gasifier: Studies on chemical kinetics and operating conditions on the performance of the biomass gasification process. Energy, 116, 1065-1076.

[54] Svishchev DA, Kozlov AN, Donskoy IG, Ryzhkov AF, (2016). A semi-empirical approach to the thermodynamic analysis of downdraft gasification, Fuel. 168, 91-106.

[55] Angelova S, Yordanova D, Kyoseva V, Dombalov I, (2014). Municipal waste utilization and disposal through gasification. Journal of Chemical Technology and Metallurgy, 49(2), 189-193

[56] Chowdhury R, Bhattacharya P, Chakravarty M, (1994). Modeling and simulation of a downdraft rice husk gasifier. International Journal of Energy Research, 18, 581–94.

[57] Roll H, Hedden K, (1994). Entrained flow gasification of coarsely ground Chinese reed. Chemical Engineering and Processing, 33(5), 353–61.

[58] Elmegaard B, Korving A, (1998). Analysis of an integrated biomass gasification/combined cycle plant. Efficiency, cost, optimization, simulation and environmental aspects of energy systems and processes. In Proceedings of the ECOS, vol. 2, Nancy, France, 1998, 591–8.

[59] Rodriguez-Alejandro DA, Nam H, Maglinao AL Jr., Capareda SC, Aguilera-Alvarado AF, (2016). Development of a modified equilibrium model for biomass pilot-scale fluidized bed gasifier performance predictions. Energy, 115, 1092-1108.

[60] Zainal ZA, Ali R, Lean CH, Seetharamu KN, (2001). Prediction of performance of a downdraft gasifier using equilibrium modeling for different biomass materials. Energy Conversion and Management, 42, 1499–515.

[61] Ahmed AMA, Salmiaton A, Choong TSY, Wan Azlina WAKG, (2015). Review of kinetic and equilibrium concepts for biomass tar modeling by using Aspen Plus. Renewable and Sustainable Energy Reviews, 52, 1623-1644.

[62] Ranzi E, Corbetta M, Manenti F, Pierucci S, (2014). Kinetic modeling of the thermal degradation and combustion of biomass. Chemical Engineering Science, 110, 2-12.

[63] Hameed S, Ramzan N, Rahman Z, Zafar M, Riaz S, (2014). Kinetic modeling of reduction zone in biomass gasification. Energy Conversion and Management, 78, 367-373.

[64] Masnadi MS, Habibi R, Kopyscinski J, Hill JM, Bi X, Jim Lim C, Ellis N, Grace JR, (2014). Fuel characterization and co-pyrolysis kinetics of biomass and fossil fuels. Fuel, 117, 1204-1214.

[65] Patra TK, Nimisha KR, Sheth PN, (2016). A comprehensive dynamic model for downdraft gasifier using heat and mass transport coupled with reaction kinetics. Energy, 116, 1230-1242.

[66] Cycle-Tempo software. http://www.asimptote.nl/software/cycle-tempo/

[67] Lemann MF, (2008). Waste Management. Peter Lang AG, Internationaler Verlag der Wissenschaften.

[68] Chao G, Yuping D, (2012). Experimental study of non woody biomass gasification in a downdraft gasifier. International Journal of Hydrogen Energy, 37(6), 4935-4944.

[69] Pérez JF, Melgar A, Benjumea PN, (2012). Effect of operating and design parameters on the gasification combustion process of waste biomass in fixed bed downdraft reactors: An experimental study, Fuel, 96, 487-496.

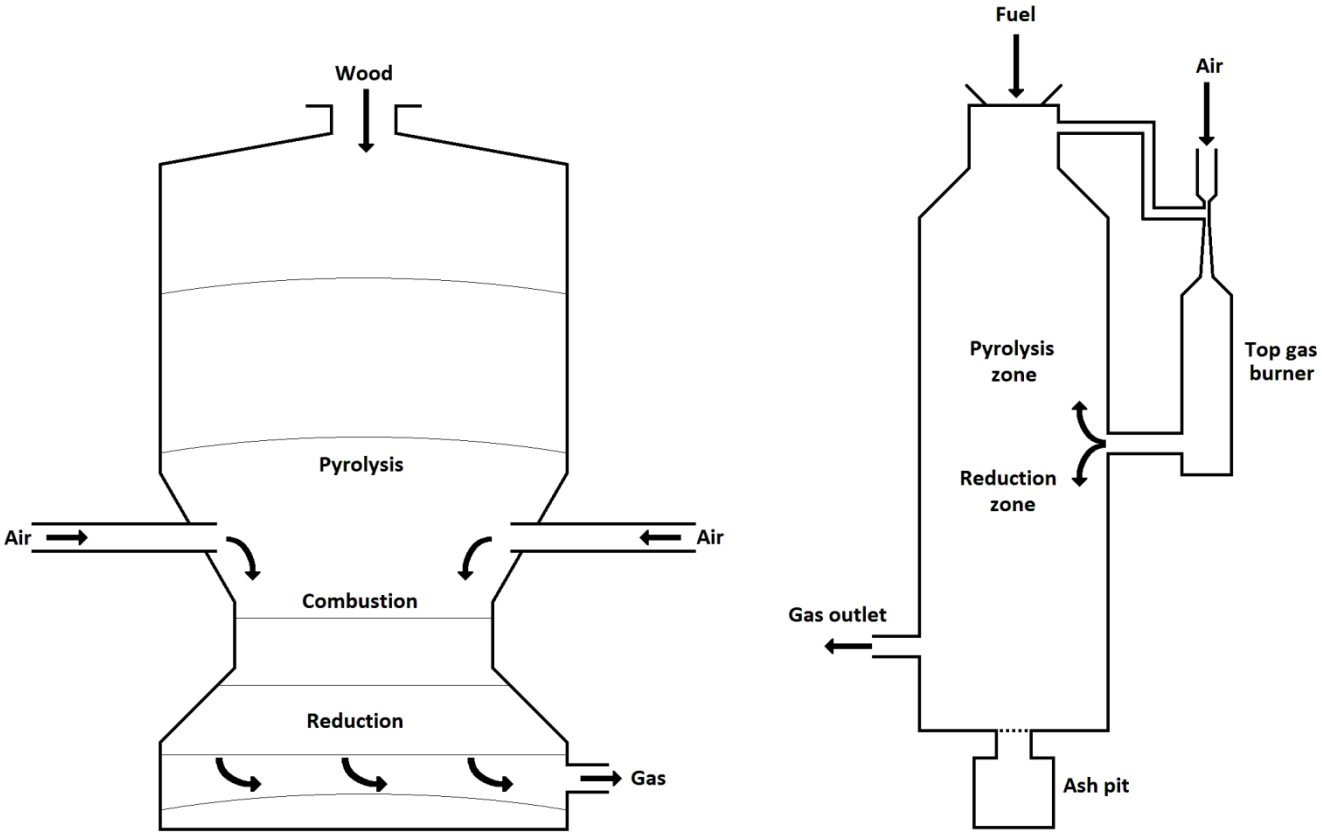

Figure 1 Sketches of downdraft gasifiers

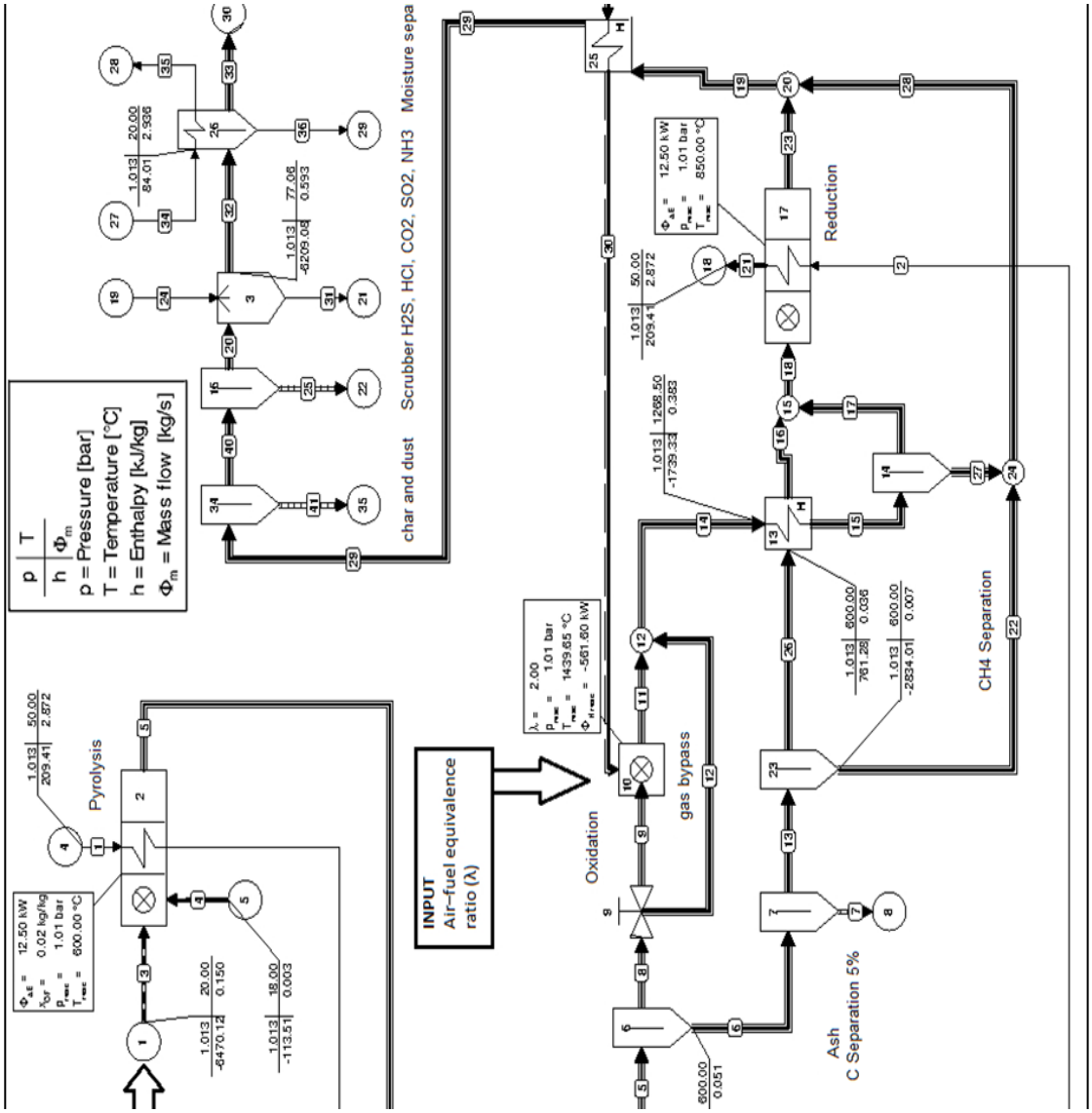

Figure 2 Layout of the downdraft gasifier model

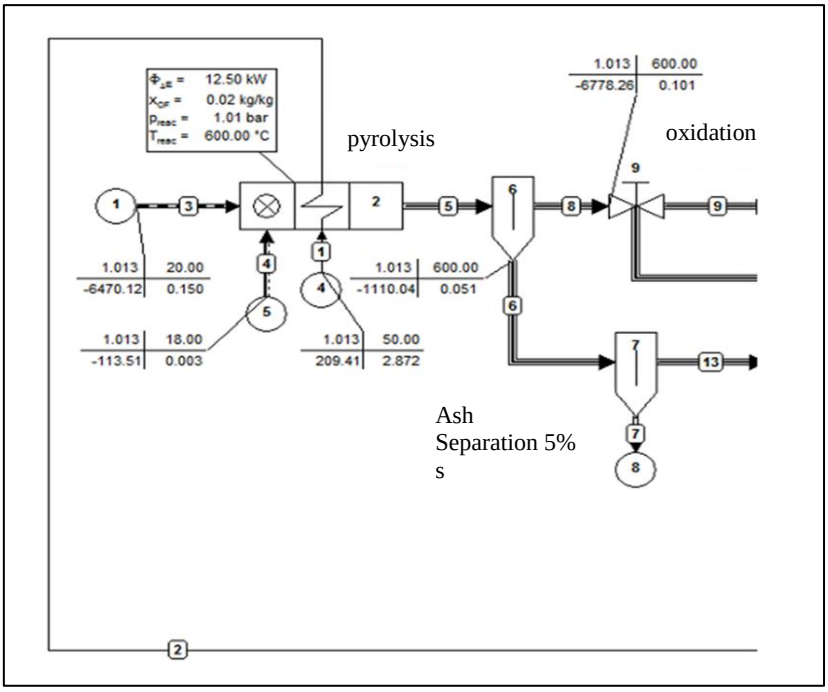

Figure 3 Part of the gasifier containing the pyrolysis module

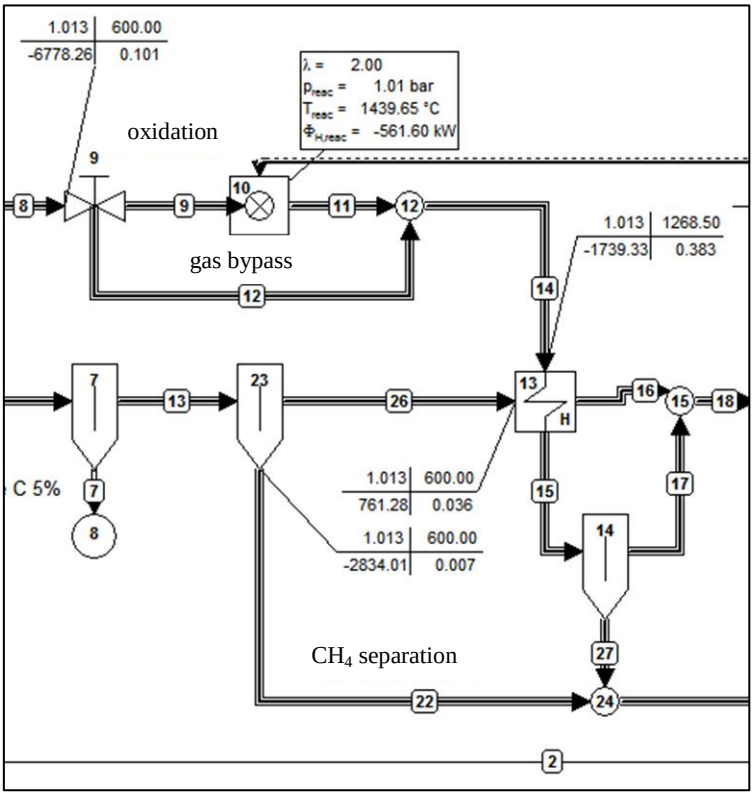

Figure 4 Part of the gasifier containing the oxidation zone

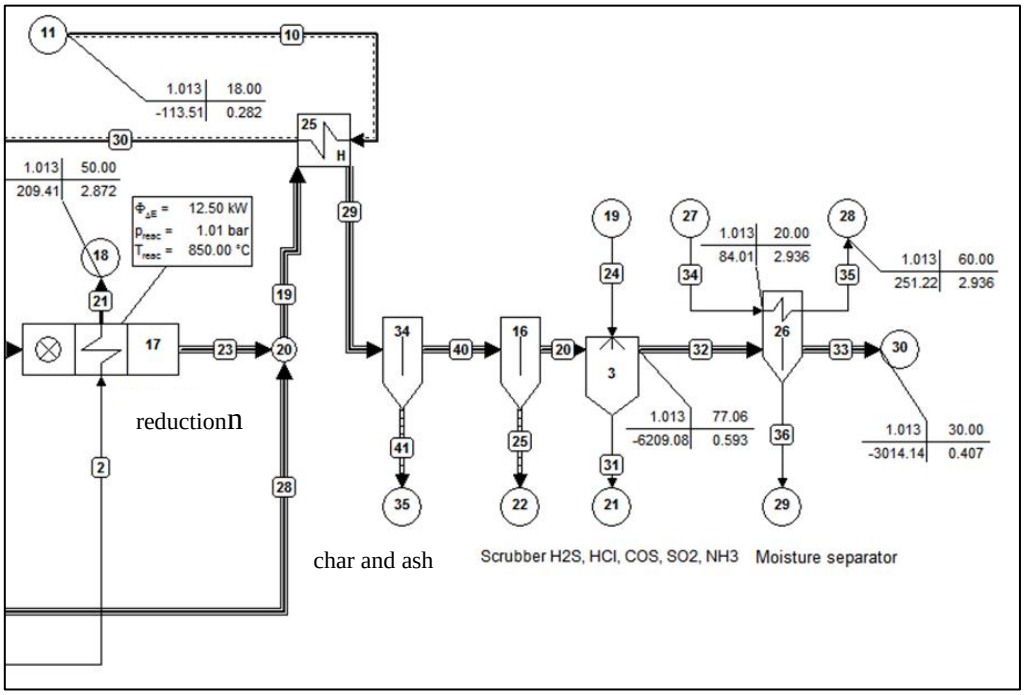

Figure 5 Last part of the gasifier model

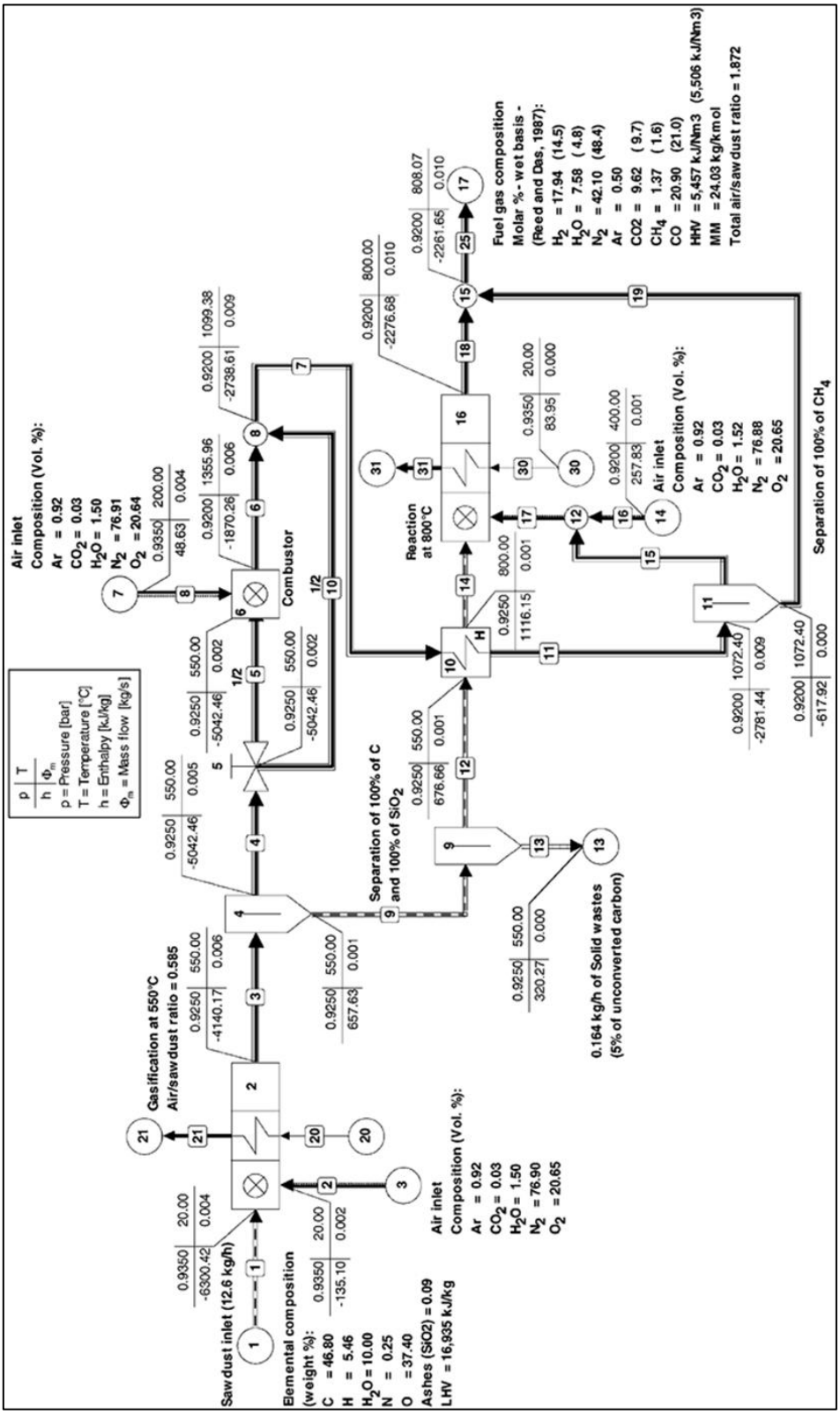

Figure 6 Layout of the Altafini's downdraft gasifier model

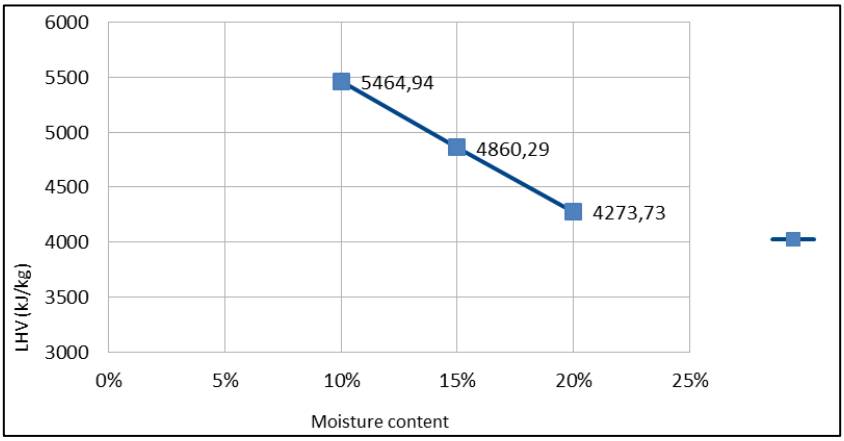

Figure 7 Low heating value versus moisture content

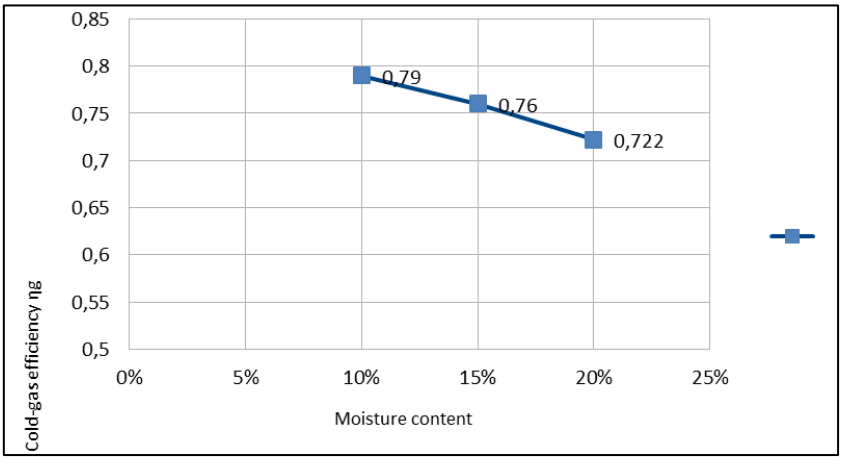

Figure 8 Cold gas efficiency versus moisture content

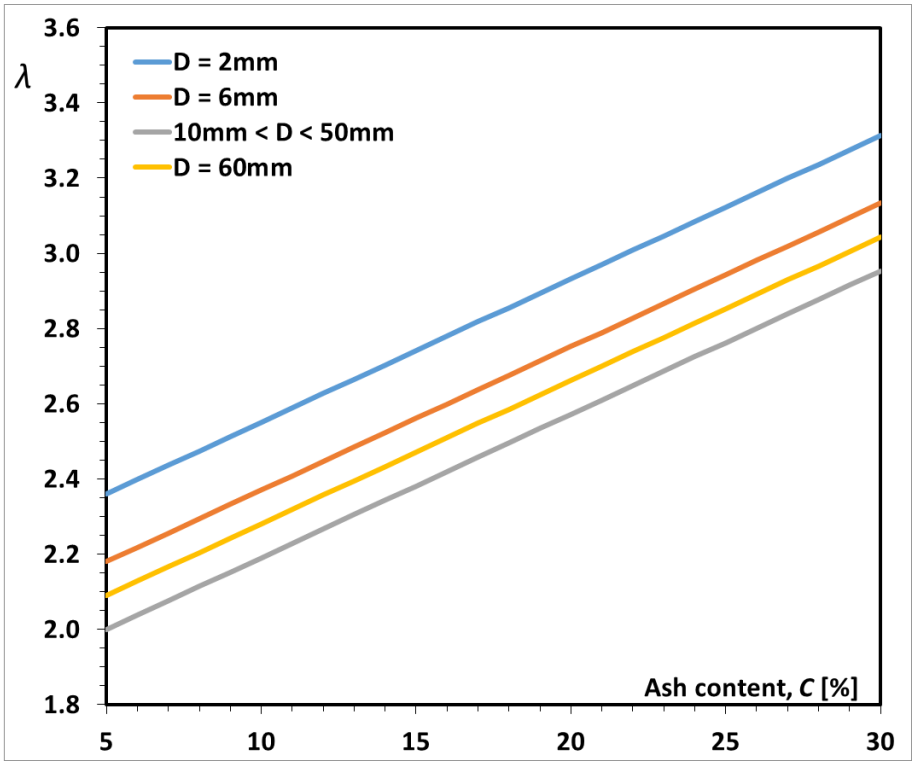

Figure 9 Equivalence ratio, λ, vs. ash content, C, at constant average particle diameters, D

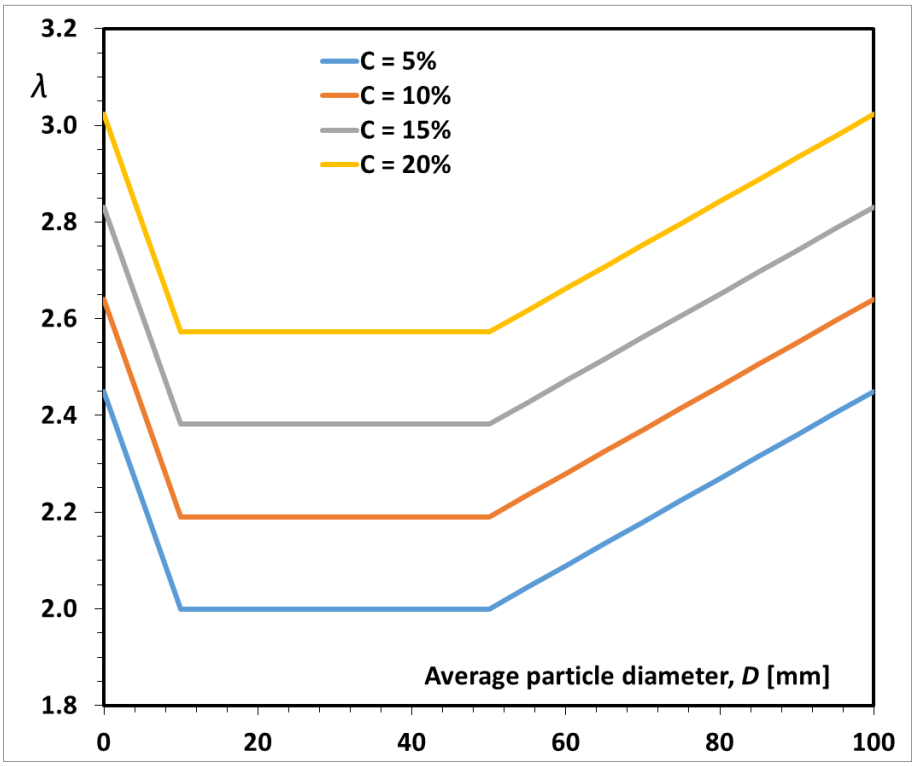

Figure 10 Equivalence ratio, λ, vs. average particle diameters, D, at constant ash content, C

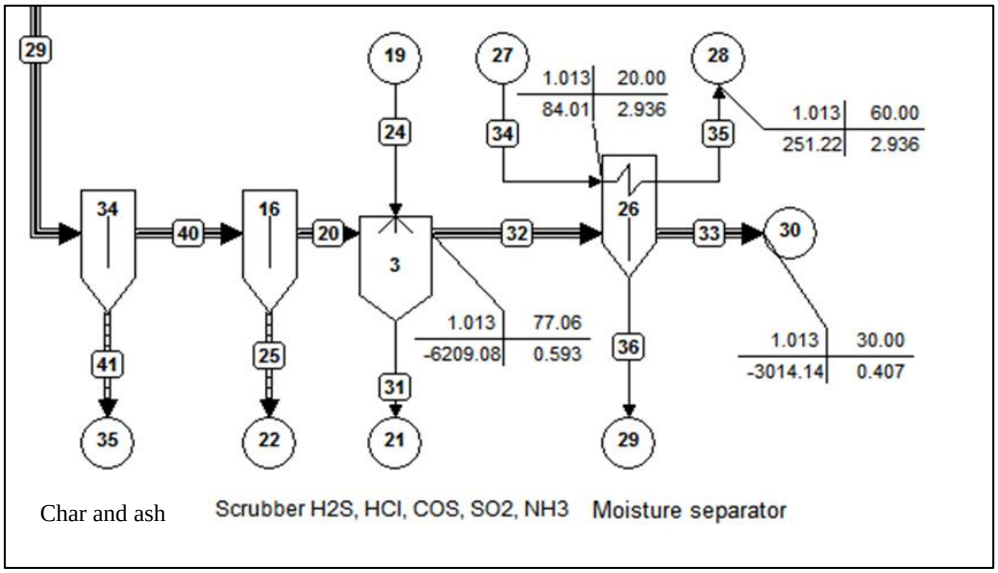

Figure 11 Gas cooling and purification system

Table 1 Composition of the pomace

Weight percentage on dry basis	C	H	O	N	S	Ash (F_2O_3, Al_2O_3, SiO_2)	Moisture	LHV (kJ/kg)
Depleted pomace	51.31	6.40	35.01	2.00	0.26	5.00	15.00	16836

Table 2 Experimental and theoretical syngas composition obtained by pomace

Syngas molar composition (%)	FB downdraft	Syngas by D. Vera (53)	Ankur experimental gasifier (53)
H_2	17.19	18.22	18(+/-)3
CH_4	3.15	1.45	Up to 3
CO	19.23	17.0	19(+/-) 3
N_2	48.70	44.5	45-50
CO_2	11.10	9.31	10(+/-) 3
H_2O	-	9.04	-
Syngas LHV (kJ/kg)	4860	4350	4400-5400
Oxidant/fuel ratio	1.88	2.21	1.5-1.8

Table 3 Theoretical composition of syngas obtained by pomace with three different moistures.

Syngas molar composition (%)	10% moisture	15% moisture	20% moisture
H_2	18.43	17.19	15.70
Ar	0.54	0.57	0.61
CH_4	3.03	3.15	3.29
CO	22.63	19.23	15.96
N_2	46.23	48.7	51.38
CO_2	9.07	11.1	13.01
H_2S	0.06	0.06	0.06
Syngas LHV (kJ/kg)	5465	4860	4274
Oxidant/fuel	1.83	1.88	1.96
Cold gas efficiency	0.79	0.76	0.72

Table 4 Composition of “leaves and pruning”, and “olive pits”

Weight percentage on dry basis	C	H	O	N	S	Ash (F_2O_3, Al_2O_3, SiO_2)	moisture	LHV (kJ/kg) on humid base
leaves and pruning	47.10	6.18	41.66	0.55	0.10	4.46	4.76	16770
Olive pits	49.62	5.81	41.76	0.47	0.04	2.30	8.80	16427

Table 5 Experimental and theoretical syngas composition obtained by “leaves and pruning” and “olive pits”

Syngas molar composition (%)	Leaves and pruning from FB downdraft	Leaves and pruning from D. Vera (53)	Olive pits from FB downdraft	Olive pits from D. Vera (53)	Ankur experimental gasifier (53)
H_2	17.77	20.40	17.52	19.86	18(+/-)3
CH_4	2.81	1.45	2.69	1.45	Up to 3
CO	22.71	21.61	23.04	21.73	19(+/-)3
N_2	45.70	40.89	45.34	40.35	45-50
CO_2	10.43	8.30	10.85	8.82	10(+/-)3
H_2O	-	6.99	-	7.27	-
Syngas LHV (kJ/kg)	5242	5270	5184	5180	4400-5400
Oxidant/fuel ratio	1.72	1.82	1.69	1.80	1.5-1.8
Cold gas efficiency	0.78	-	0.79	-	Up to 0.85

Table 6 Physical properties of sludge and sawdust

	Ankur gasifier	Sludge	Sawdust	Sawdust variations	Sludge variations
Particle diameter (mm)	10-50 mm	35 mm	2-3 mm	-80%	0
Ash content	<5%	20.73	0.10	0	+314.6%
Value of λ used	2	2.60	2.36	+18%	+30%

Table 7 Composition of “sawdust”

Weight percentage on dry basis	C	H	O	N	S	Ash (F_2O_3, Al_2O_3, SiO_2)	moisture	LHV (kJ/kg) on humid base
Sawdust	52.0	6.07	41.55	0.28	-	0.10	10	16935

Table 8 Experimental and theoretical syngas composition obtained by “sawdust”

Syngas molar composition	FB downdraft	Experimental gasifier – Altafini (51)	Relative difference (%)
H_2	14.95	14	6.8%
CH_4	2.60	2.31	12.6%
CO	19.45	20.14	-3.4%
N_2	50.23	50.79	-1.1%
CO_2	12.16	12.06	0.8%
H_2O	-	-	
Syngas HHV (kJ/Nm^3)	5259	5276	-0.3%
Oxidant/fuel ratio (Nm^3/kg)	2.07	1.829	13.2%
Cold gas efficiency	0.73	0.629	16.1%

Table 9 Composition of “sewage sludge”

Weight percentage on dry basis	C	H	O	N	S	Ash (F_2O_3, Al_2O_3, SiO_2)	Moisture	LHV (kJ/kg) on humid base
Sewage sludge	39.48	6.19	25.46	3.93	1.45	23.51	11.75	14893.70

Table 10 Experimental and theoretical syngas composition obtained by “sewage sludge”

Syngas molar composition	FB downdraft	Experimental gasifier – Dogru et al. (58)	Relative difference (%)
H_2	10.30	8.80 … 11.15	17.0% … -7.6%
CH_4	3.20	2.07	54.6%
CO	9.77	9.2 … 10.63	5.3% … -8.1%
N_2	61.86	62 … 64.41	-0.2% … -4.0%
CO_2	13.78	11.11 … 13.24	24.0% … 4.1%
H_2O	-	-	-
Syngas HHV (kJ/Nm^3)	3864	3820	1.2%
Oxidant/fuel ratio (Nm^3/kg)	2.0	2.28 … 2.69	-12.3% … -25.7%
Cold gas efficiency	0.567	0.62 … 0.64	-8.5% … -11.4%

Table 11 Physical properties of RDF

	Ankur gasifier	RDF	RDF variations
Particle diameter (mm)	10-15 mm	7 mm	-30%
Ash content (on humid base)	<5%	11.04	+120.8%

Table 12 RDF composition

Weight percentage on dry basis	C	H	O	N	S	Cl	Ash (F_2O_3, Al_2O_3, SiO_2)	moisture	LHV (kJ/kg) on humid base
RDF (59)	48.23	6.37	28.48	1.22	0.76	1.13	13.81	20	12900

Table 13 Experimental and theoretical syngas composition obtained by RDF

Syngas molar composition (%)	FB downdraft	Fix bed downdraft gasifier (59)	Relative difference (%)
H_2	10.55	7 … 9	50.7% … 17.2%
CH_4	2.82	6 … 9	-53.0% … -68.7%
CO	10.20	9 … 13	13.3% … -21.5%
N_2	49.93	4 ... 52	1148.3% … -4.0%
CO_2	12.04	12 … 14	0.3% … -14.0%
H_2O	13.52	10 … 14	35.2% … -3.4%
Syngas LHV (kJ/kg)	3037	-	-
Oxidant/fuel ratio	2.31	-	-
Cold gas efficiency	0.75	-	-

Table 14 Composition of corn straw

Weight percentage on dry basis	C	H	O	N	S	Cl	Ash (F_2O_3, Al_2O_3, SiO_2)	moisture	LHV (kJ/kg) on humid base
Mais	43.38	5.95	45.01	0.97	0.13	0.49	5.93	6.17	14903

Table 15 Physical properties of corn straw

	Ankur gasifier	Corn straw	Corn straw variations
Particle diameter (mm)	10-50 mm	3.75 mm	-62.5%
Ash content (on humid base)	<5%	5.91	+18.2%

Table 16 Experimental and theoretical syngas composition obtained by corn straw

Syngas molar composition (%)	FB downdraft	Experimental gasifier (Gai et al.)
H_2	13.25	6.91-13.51
CH_4	2.62	1.27-3.96
CO	15.90	11.35-19.81
N_2	52.83	48.58-59.71
CO_2	14.72	11.58-23.93
H_2O	-	-

Table 17 Experimental and theoretical composition of the purified syngas, derived by pomace according to Gai et al.

Syngas molar composition (%)	FB downdraft	Experimental gasifier - Gai et al. (12)	Relative difference (%)
H_2	13.25	6.91 … 13.51	91.8% … -1.9%
CH_4	2.62	1.27 … 3.96	106.3% … -33.8%
CO	15.90	11.35 … 19.81	40.1% … -19.7%
N_2	52.83	48.58 ... 59.71	8.7% … -11.5%
CO_2	14.72	11.58 … 23.93	27.1% … -38.5%
H_2O	-	-	-
Syngas LHV (kJ/kg)	4317	2690 … 5390	60.5% … -19.9%
Oxidant/fuel ratio	1.49	1.29 … 2.88	15.5% … -48.3%
Cold gas efficiency	0.75	-	-